

Electronic Structure and Optical Limiting Behavior of Carbon Nanotubes

P. Chen, X. Wu, X. Sun, J. Lin,* W. Ji, and K. L. Tan

Physics Department, National University of Singapore, Singapore 119260

(Received 2 June 1998)

Carbon nanotubes prepared by catalytic (CO) disproportionation were studied using TEM, XRD, UPS, XPS, and optical spectroscopies. In comparison with graphite, the carbon nanotubes show greater interplanar distance, smaller work function, steeper Fermi edge, negative core-level shift, and stronger plasma excitation. Their valence band is basically the same as that of graphite, with lower intensity in the binding energy region of 2–7 eV. The carbon nanotubes exhibit a strong optical limiting effect, superior to both carbon black and C₆₀. [S0031-9007(99)08764-5]

PACS numbers: 71.20.Tx, 61.48.+c, 78.20.-e

Carbon nanotubes possess many unique properties and can be used for 1D quantum wires, optical switchers, nano-transistors, and other essential electronic components. They have been recognized as a fascinating material about to trigger a revolution in nanodevices, optical computing, optical communication, carbon chemistry, and new functional structural materials, generating intense research activities in recent years [1–8]. In regard to their electronic and optical properties, many of the investigations were theoretical predictions, with few experimental measurements reported so far. In this paper, transmission electron microscopy (TEM), x-ray diffraction (XRD), ultraviolet photoemission spectroscopy (UPS), x-ray photoemission spectroscopy (XPS), and nonlinear optical studies were applied to determine the atomic arrangement, electronic structure, and nonlinear optical properties of carbon nanotubes.

The carbon nanotubes in this investigation were prepared by catalytic CO disproportionation, which has been developed to be able to produce highly (>95%) purified tubes in desired sizes ranging from 7 to 35 nm under control, as described elsewhere [9]. XRD measurements were conducted on a Philips PW 1710 diffractometer. UPS and XPS investigations were performed on a VG ESCALAB Mk II machine, using He I (21.2 eV), He II (40.8 eV) resonance lines, and Mg *K*α (1254.6 eV) as ionization sources, respectively. The binding energy values reported below are all referenced to the Fermi level. Low-resolution TEM and electron diffraction studies were conducted on a JEM-100CX electron microscope. High-resolution TEM observation was carried out on a Philip FEG CM300 electron microscope. Optical absorption spectra in the visible region were recorded on a Hitachi UV-3410 spectrophotometer, while nonlinear transmission measurements were made using laser pulses of 7-ns duration produced by a *Q*-switched Nd:YAG laser or a dye laser. To generate 532-nm laser pulses or pump the dye laser, a second-harmonic-generation crystal was used. The lasers were operated in single-shot mode. The laser beam was focused on samples with a spot radius of ~30 μm.

As observed by TEM, the sample in this study is composed of carbon nanotubes, which are small and even in

size (diameter 15–20 nm), consisting of multilayers of graphene sheets, rolled up like a hollow cylinder. Little (<5%) non-nanotube materials such as metal (catalyst) particles, amorphous carbon, disordered carbon, etc. were observed from careful TEM inspection as well as high temperature hydrogen etching. The XRD pattern (not shown here) of the carbon nanotubes is similar to that of graphite [though the main peak (002) is much weaker and broadened], indicating that the hexagonal ring structure of graphene sheets remains unchanged in the carbon nanotubes. The shift of the (002) reflection from $2\theta = 26.4^\circ$ for graphite to 25.6° for the carbon nanotubes reveals an increase in the interlayer distance from 0.335 nm for graphite to 0.347 nm for the carbon nanotubes. This result has been confirmed by the electron diffraction measurements of the same sample. Annealing at 1370 K has shown an enhanced crystallinity of the carbon nanotube sample. The (101) reflection of the annealed carbon nanotubes can become fairly strong and even sharper than that of graphite.

Figure 1 displays the UPS He II spectra obtained from the annealed carbon nanotubes and graphite. As expected, the valence band structure of carbon nanotubes is basically the same as that of graphite. Nevertheless, the intensity in the binding energy (BE) region between 2.0 and 7.6 eV is noticeably lower for the nanotubes than graphite. According to previous photoemission spectroscopic data and theoretical band structure calculations for graphite [10], this energy region is assigned to $2p-\pi$, which overlaps with the top of $2p-\sigma$ and is contributed by the graphene $2p-\pi$ electrons. The reduction in the $p\pi$ electron density for carbon nanotubes is thus understandable, resulting from the curvature of graphene sheets. A small increase in the intensity around a BE of 11.5 eV, which is attributed to $p-\sigma$ contribution [10], can be simultaneously observed in Fig. 1. This is further evidence of the $\sigma-\pi$ hybridization effect resulting from the formation of carbon tubes [8].

Theoretical calculations [6,8,11] have predicted that in certain cases, depending on the size of carbon nanotubes, the energy gap of carbon nanotubes may become almost zero and some density of state appear near the Fermi

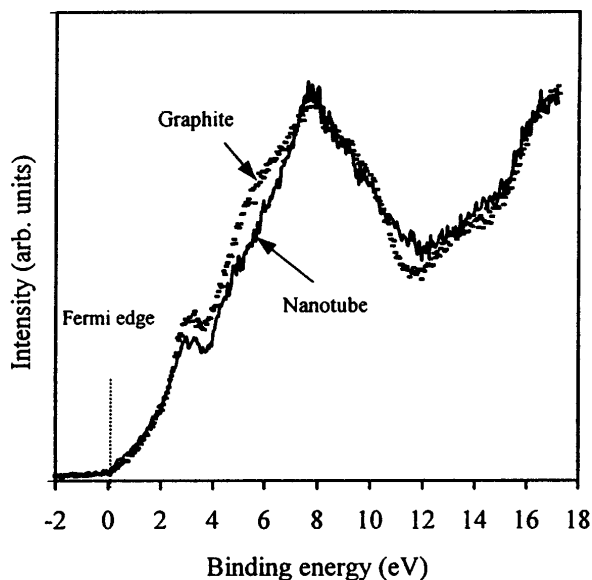


FIG. 1. UPS He II valence band spectra of the carbon nanotubes (solid line) and graphite (dotted line).

level. We have indeed observed these changes in carbon nanotubes by measuring and comparing the threshold of the secondary electron tail and the Fermi edge in the He I spectra for the carbon nanotubes and graphite samples. As shown in Fig. 2, the secondary electron tail threshold is shifted to higher binding energy by 0.2 eV while a steeper Fermi edge is detected for the carbon nanotubes as compared with graphite. Since in UPS He I spectra the vacuum level can be determined at the position 21.2 eV apart from the secondary electron tail threshold, the 0.2 eV shift of the secondary electron cutoff means

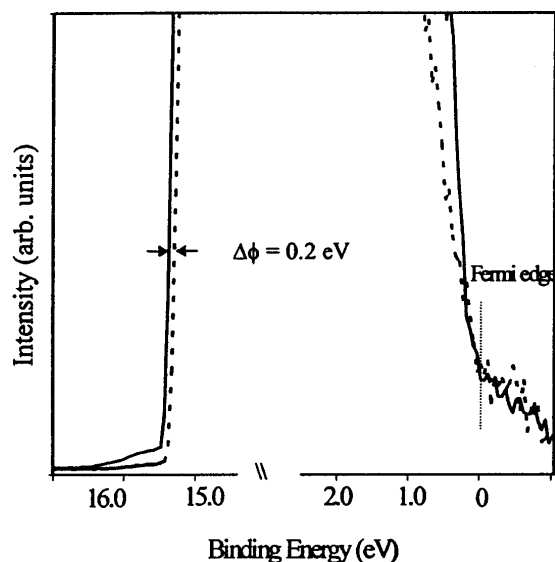


FIG. 2. The secondary electron tail threshold and the Fermi edge for the carbon nanotubes (solid line) and graphite (dotted line), determined by He I UPS.

a 0.2 eV decrease in the nanotubes' work function; i.e., their work function is closer to the Fermi level by 0.2 eV than that of graphite. This change is regularly observable for carbon nanotubes of various sizes in our studies. The lower work function of carbon nanotubes compared with that of graphite was recently reported in a conference document, relying on theoretical and thermal electron emission studies on carbon nanotube thin films [12].

The XPS study has also revealed the difference between graphite and the carbon nanotubes in the C 1s core level energy position, full width at half maximum (FWHM), and its energy loss fine structures. As usual, the C 1s peak is detected at a BE of 284.6 eV for graphite. It shifts to lower binding energy by 0.3 eV for carbon nanotubes, with a larger FWHM of 1.1 vs 1.0 eV of graphite. The negative shift of the C 1s peak may be ascribed to weaker *c-c* binding caused by the curvature of graphene sheets as well as the larger interlayer distance of the carbon nanotubes. Again the larger FWHM is regularly observed for carbon nanotubes of various diameters, and may indicate a shorter lifetime of the holes of C 1s photoemission in nanotubes in comparison to that of graphite. Figure 3 is the normalized XPS C 1s core-energy-loss spectra for the carbon nanotubes and graphite. They demonstrate a sharp peak at ~ 6.6 eV loss energy and a very broad loss feature around 27 eV, corresponding to collective π and $\sigma + \pi$ plasma excitation, respectively [13–15]. In comparison with those of graphite, both (low- and high-energy transition) loss features are stronger for carbon nanotubes, in good agreement with those previously reported [14]. This

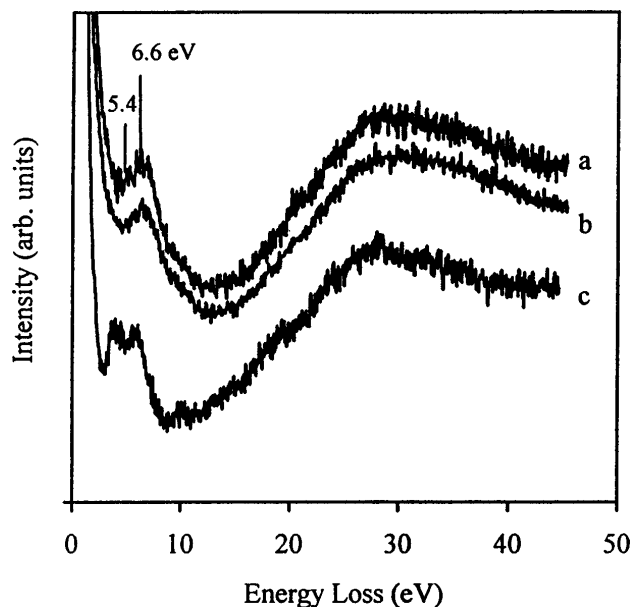


FIG. 3. The C 1s core-energy-loss spectra for (a) the carbon nanotubes; (b) graphite; and (c) C₆₀. The spectra have been normalized to the C 1s main peak and relocated with the loss energy of the main peaks all being zero. The spectrum of C₆₀ is moved down for clear presentation.

appears to be related to the curved nature of the graphene sheets in carbon nanotubes. In graphite, the carbon $2p$ - π electron density is symmetrically distributed with respect to the flat graphene plane, whereas in nanotubes it is relocalized with most of the wave function being outside the curved graphene layers, which is favorable to π electron plasma transitions [11]. In addition to the above difference in the intensity of loss features, some extra low-energy transitions (π electron plasmon) are observable at ~ 5.4 eV for carbon nanotubes. This phenomenon is also observable and most evident on C_{60} samples [see Fig. 3(c)]. The energy position of the π plasma loss peak is known to be related to the delocalization of $2p$ - π electrons. According to the literature [15], the dispersion coefficient of $2p$ - π electrons is 0.5 for graphite and 0.25 for C_{60} . It can be estimated that the corresponding coefficient for carbon nanotubes would be between 0.25 and 0.5.

Figure 4 displays the optical limiting behavior of the carbon nanotubes (in diameters between 15 and 20 nm) suspended in ethanol, measured with 532-nm [see the open circles in Fig. 4(a)] and 1064-nm [Fig. 4(b)] laser pulses. At incident fluences of less than 0.06 J/cm² the energy transmittance is a constant. However, in excess of 0.06 J/cm², the transmittance decreases as the incident fluence increases, a typical limiting property. Experiments have been performed on the carbon nanotubes with different diameters (e.g., 5–10 nm, 15–20 nm, and 25–35 nm), producing similar results under the identical conditions (see Fig. 5). For a comparison, Fig. 4 also shows the nonlinear limiting effect of the C_{60} dissolved in toluene solution (the crosses) and the carbon black which is aggregates of small carbon particles suspended in distilled water (the solid triangles). The ex-

periments have been conducted under the same conditions, while the concentration of the C_{60} and carbon black in the tested solutions has been adjusted in such a way that its linear transmittance is $\sim 50\%$ at 532 nm, close to that of the carbon nanotubes. In Fig. 4, the linear transmittance is normalized to unity to facilitate the comparison. The limiting threshold, defined as the incident fluence at which the transmittance falls to half of the linear transmittance, is around 1.0 J/cm² for the carbon nanotubes, lower than those of C_{60} and carbon black as shown in Fig. 4(a). Figure 4(b) clearly demonstrates that the carbon nanotubes are a broadband limiter up to 1064 nm (inclusive of 700 nm, though the data are not shown), whereas at 1064 nm carbon black has much higher threshold value, and limiting phenomena totally vanish for the C_{60} solution. In C_{60} , excited state absorption has been identified as a dominant mechanism for optical limiting [16]. Indeed the optical absorption spectrum in the inset of Fig. 4(a) does show a ground-state absorption at 532 nm for C_{60} . The ground-state absorption promotes electrons into excited states, giving rise to the excited-state absorption. No ground-state absorption at 1064 nm in the inset of Fig. 4(a) explains why there is no limiting response from C_{60} at this wavelength. For the carbon nanotubes, the ground-state absorption is absent at 532 and 1064 nm. On the other hand, our electronic structure study discussed above shows that the carbon nanotubes have a lower work function, lower electron binding energy, and stronger plasma excitation. These and the broadband limiting response appear to suggest that the limiting property of the carbon nanotubes may mainly result from another mechanism, i.e., nonlinear scattering, which has been identified

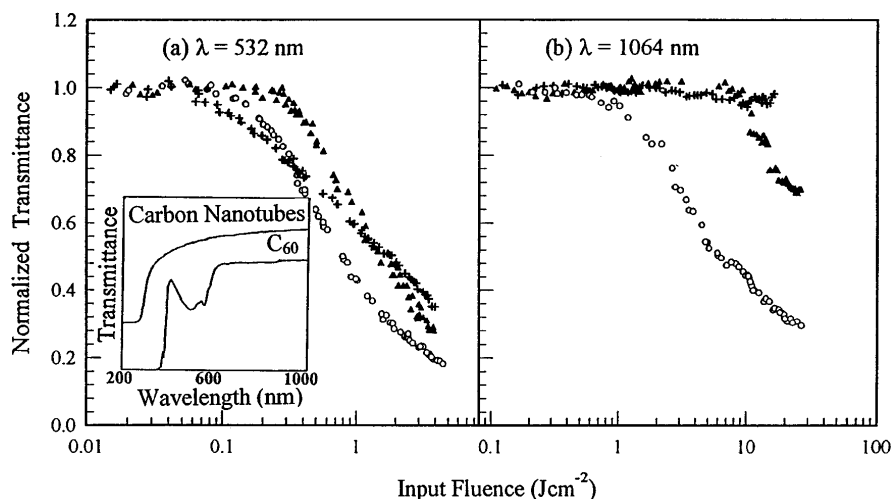


FIG. 4. Nonlinear transmission of the carbon nanotubes in ethanol (\circ); C_{60} in toluene ($+$); and carbon black in distilled water (\blacktriangle). The nonlinear transmission was measured with 7-ns laser pulses at (a) 532-nm, and (b) 1064-nm wavelength. The linear transmittance of the three systems has all been normalized to unity. The inset of (a) shows the optical transmission spectra recorded in the wavelengths between 200 and 1200 nm for the carbon nanotubes suspended in ethanol (top curve) and C_{60} dissolved in toluene (bottom curve). The transmission spectrum of the nanotubes has been shifted vertically for clear presentation. The spectrum of the carbon black suspension is identical to that (the top curve) of the carbon nanotubes.

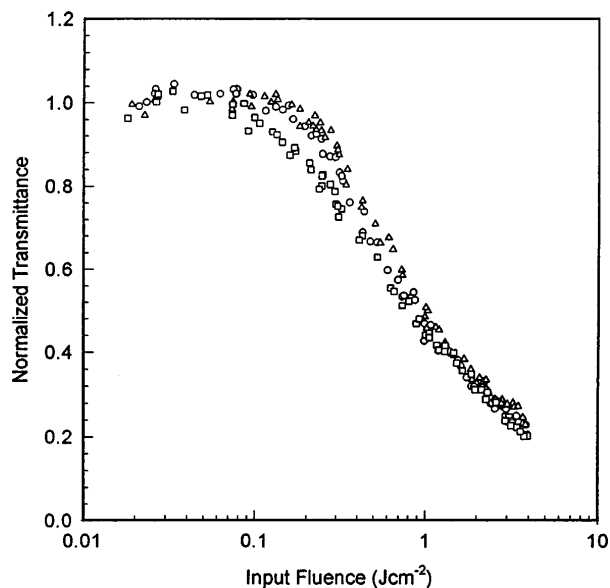


FIG. 5. Nonlinear transmission of the carbon nanotubes in ethanol, measured with 7-ns laser pulses at 532 nm for carbon nanotubes with diameter of 5–10 nm (\square), 15–20 nm (\circ), and 25–30 nm (\triangle).

to be the dominant process for carbon black suspensions [17–19]. In this process, heating due to the presence of the laser pulses can lead to vaporization and ionization of carbon particles or nanotubes, and then form rapidly expanding microplasmas. In return, these microplasmas strongly scatter light from the transmitted beam direction, leading to the decrease in the measured transmitted light energy. The carbon black in this study was observed (by TEM) to consist of carbon particles in the size similar to that of our carbon nanotubes, and its linear transmittance was adjusted to the same level of the carbon nanotubes. Hence, though it is still difficult to understand the difference between the behavior of carbon black and nanotubes, the excellent optical limiting effect of the carbon nanotubes may be related to their stronger plasma excitation, lower electron binding energy, and lower work function as discussed previously.

*To whom correspondence should be addressed.

Email address: phylinjy@nus.edu.sg

- [1] S. J. Tans, M. H. Devoret, H. Dai, A. Thess, R. E. Smalley, L. J. Geerligs, and C. Dekker, *Nature (London)* **386**, 474 (1997).
- [2] M. Bockrath, D. H. Cobden, P. L. McEuen, M. G. Chopra, A. Zettl, A. Thess, and R. E. Smalley, *Science* **275**, 1922 (1997).
- [3] Thomas W. Ebbesen, *Carbon Nanotubes* (CRC Press, Boca Raton, Florida, 1997).
- [4] M. Endo, S. Iijima, and M. S. Dresselhaus, *Carbon Nanotubes* (Pergamon, Oxford, 1996).
- [5] P. G. Collins, A. Zettl, H. Bando, A. Thess, and R. E. Smalley, *Science* **278**, 100 (1997).
- [6] N. Hamada, S. Sawada, and A. Oshiyama, *Phys. Rev. Lett.* **68**, 1579 (1992).
- [7] R. Saito, M. Fujita, G. Dresselhaus, and M. S. Dresselhaus, *Phys. Rev. B* **46**, 1804 (1992).
- [8] L. X. Benedict, S. G. Louie, and M. L. Cohen, *Phys. Rev. B* **52**, 8541 (1995).
- [9] P. Chen, H. B. Zhang, G. D. Lin, Q. Hong, and K. R. Tsai, *Carbon* **35**, 1495 (1997).
- [10] F. R. McFeely, S. P. Kowalczyk, L. Ley, R. G. Cavell, R. A. Pollak, and D. A. Shirley, *Phys. Rev. B* **9**, 5268 (1974).
- [11] X. Blasé, L. X. Benedict, E. L. Shirley, and S. G. Louie, *Phys. Rev. Lett.* **72**, 1878 (1994).
- [12] Y. V. Gulyaev *et al.*, in *Proceedings of the 9th International Vacuum Microelectron Conference, St. Petersburg, Russia, 1996* (IEEE, New York, 1996).
- [13] V. P. Dravid, X. Lin, Y. Wang, X. K. Wang, A. Yee, J. B. Ketterson, and R. P. H. Chang, *Science* **259**, 1601 (1993).
- [14] P. M. Ajayan, S. Iijima, and T. Ichihashi, *Phys. Rev. B* **47**, 6859 (1993).
- [15] J. Fink, Th. Muller-Heinzerling, J. Pfluger, and B. Scheerer, *Phys. Rev. B* **30**, 4713 (1984).
- [16] See, for example, D. G. Mclean, R. L. Sutherland, M. C. Brant, D. M. Brandelik, P. A. Fleitz, and T. Pottenger, *Opt. Lett.* **18**, 858 (1993).
- [17] K. Mansour, M. J. Soileau, and E. W. Van Stryland, *J. Opt. Soc. Am. B* **9**, 1100 (1992).
- [18] K. M. Nashold and D. P. Walter, *J. Opt. Soc. Am.* **12**, 1228 (1995).
- [19] R. Goedert, R. Becker, A. Clements, and T. Whittaker III, *J. Opt. Soc. Am. B* **15**, 1442 (1998).